

# Study of third-order optical non-linearity and electrical conductivity of sol-gel processed silica: poly(2-bromo-5-methoxy-*p*-phenylene vinylene) composite

Chichang J. Wung, Kwang-Sup Lee and Paras N. Prasad\*

Photonics Research Laboratory, Department of Chemistry, State University of New York at Buffalo, Buffalo, NY 14214, USA

and Jong-Chul Kim and Jung-Il Jin

Department of Chemistry, Korea University, Seoul 136-701, Korea

and Hong-Ku Shim

Department of Chemistry, Korea Advanced Institute of Science and Technology, Taejeon 305-701, Korea

(Received 29 November 1991; accepted 27 January 1992)

A novel sol-gel processed silica: poly(2-bromo-5-methoxy-*p*-phenylene vinylene)/silica composite was prepared using a soluble precursor. The optical properties of this material have been investigated using u.v.-visible and FTi.r. spectroscopy. The densification process was monitored by d.s.c. and t.g.a. The third-order non-linear susceptibility  $\chi^{(3)}$  has been investigated for both the pure polymer and its sol-gel composite at 602 nm using femtosecond degenerate four-wave mixing. A relatively large  $\chi^{(3)}$  value with a subpicosecond response is observed. The electrical conductivities of AsF<sub>5</sub> doped polymer and composite films were studied using four-probe measurement.

(Keywords: sol-gel; composite; poly(*p*-phenylene vinylene); non-linear optics)

## INTRODUCTION

Recently the sol-gel process for making organic/inorganic composites has received significant attention from material scientists. Specifically, there has been increased interest in these materials as optical layers for advanced photonics applications. One of the most important material properties in photonics is the non-linear optical effect because of its importance for optical signal processing<sup>1-4</sup>. Conjugated polymers containing extensive  $\pi$ -electron delocalization have emerged as an important class of third-order non-linear optical materials because of the large  $\pi$ -electron contribution to the optical non-linearity<sup>1</sup>. The non-linear optical response time for these materials has been shown to be in the subpicosecond region<sup>1</sup>. The large optical non-linearity and the fast response time mean that conjugated polymer systems are of great importance in optical signal processing. Unfortunately, most organic polymers have generally not been found to be good photonic media due to high optical losses. Inorganic glasses, however, are excellent photonic media because of their high optical quality and extremely low optical losses. Therefore, combining inorganic glass and

organic polymer is one of the best ways to obtain materials with large non-linearity and low optical losses.

Sol-gel methods have been actively studied as possibly superior routes for the preparation of ceramics, glasses and composites<sup>5-7</sup> due to the potential advantages<sup>7-10</sup> and uniqueness of this process compared to conventional melt/sintering techniques. Since the sol-gel process involves the use of low viscosity solutions as the starting reagents, there are several clear advantages: (i) high degree of homogeneity, (ii) better control of stoichiometry; (iii) low processing temperature, (iv) less contamination and (v) ease of preparation of thin films.

Generally speaking, the sol-gel composites can be made either by cogelation of monomers or oligomers with alkoxide or by impregnation in porous gels. Nevertheless, not all polymers can form a sol-gel composite by cogelation or impregnation with alkoxide. We have developed a new route for preparing optical quality composite by mixing the precursor polymer with the inorganic glass precursor and conversion to final polymer/silica composite by thermal treatment. This process is suitable when the polymer is processible through a suitable precursor polymer which can be dissolved together with the alkoxide in a common solvent without any phase separation or precipitation.

\* To whom correspondence should be addressed

The first successful polymer/silica composite made from the precursor technique was developed in the Photonics Research Laboratory at Buffalo<sup>11</sup>. In order to obtain both a high non-linear coefficient  $\chi^{(3)}$  and a high optical quality composite one of the large  $\chi^{(3)}$  conjugated polymers, poly(*p*-phenylene vinylene) (PPV), and silica alkoxide were mixed successfully without any phase separation or precipitation<sup>12</sup>. This very special composite has shown great advantages in the optical waveguiding and photonic applications<sup>13-15</sup>. Since PPV and one of its derivatives, poly(2-bromo-5-methoxy-*p*-phenylene vinylene) (designated as BrMPPV), can be prepared by precursor techniques<sup>16,17</sup>, the processing of an inorganic oxide and  $\pi$ -conjugated organic polymers via this technique became possible. In this paper, another successful process is reported for preparing an optical polymer composite material made of BrMPPV and silica glass by employing the sol-gel technique. The choice of BrMPPV in this process was based on two factors: the processibility of this polymer through the precursor technique; and the non-resonant third-order susceptibility  $\chi^{(3)}$  is predicted to be greater than that of PPV because of the electron donor substituents at the 2 and 5 positions. The preparation of this composite by the sol-gel process, the optical and electrical properties measurements of this composite and the  $\chi^{(3)}$  measurements by the degenerate four-wave mixing (DFWM) technique are discussed.

## EXPERIMENTAL

### *Synthesis of BrMPPV*

The BrMPPV precursor was prepared using the procedure described elsewhere<sup>17</sup>. For comparison PPV and poly(2-methoxy-5-butoxy-*p*-phenylene vinylene) (BuMPPV) were also prepared by the precursor technique as reported elsewhere<sup>16,18</sup>.

### *Sol-gel process*

The BrMPPV/sol-gel composite was produced by mixing the sulphonium polyelectrolyte polymer precursor for BrMPPV and tetramethyl orthosilicate (TMOS) (Aldrich) in a common solvent. Since the common solvent for BrMPPV and PPV precursor is methanol, the preparation of the BrMPPV/sol-gel composite is the same as that for the PPV/sol-gel composite which is described elsewhere<sup>12,13</sup>. Soon after the BrMPPV/sol-gel silica precursor solution is formed, the solution is cast on a suitable substrate (microscope slide or quartz plate) using either the spin coating or the doctor blading technique. The precursor films are then thermally treated with the temperature increased at a rate of  $20^\circ\text{C min}^{-1}$  in a vacuum oven ( $\sim 1.33$  Pa) and held at  $210^\circ\text{C}$  for 20 h. As a result, the BrMPPV precursor is converted into BrMPPV and an optical quality composite film is formed.

### *Band gap measurements*

In order to qualitatively relate  $\chi^{(3)}$  with the band gap for a compound, the u.v.-visible spectra for BrMPPV and the BrMPPV/sol-gel composite were obtained from the films cast on a quartz plate and compared with PPV, the PPV/sol-gel composite and its derivatives. A Shimadzu spectrophotometer (model 3101 PC) was used. The band gap energies were determined by the onsets of the absorption positions in the spectra.

### *Refractive index and film thickness measurements*

The refractive index and thickness of the film were determined by a Prism Coupler (Metricon PC-2000). The basic theory for this instrument is based on the waveguide technique. The sample to be measured is brought into contact with the base of a prism by means of a pneumatically operated coupling head, creating a small air gap between the film and the prism. A laser beam strikes the base of the prism and is normally totally reflected at the prism base onto a photodetector. However, at certain discrete values of the incident angle  $\theta$ , called mode angles, photons tunnel across the air gap into the film and enter into a guided optical propagation mode, causing a sharp drop in the intensity of light reaching the detector.

### *Measurement of $\chi^{(3)}$*

The experimental set-up used for DFWM utilized a laser system in which the i.r. output of a mode-locked continuous wave (CW) Nd:YAG laser (Spectra Physics, model 3800) is first compressed in a grating fibre compressor (Spectra Physics, model 3690) and then frequency-doubled to sync-pump a CW dye laser (Spectra Physics, model 375). The dye pulses are subsequently amplified by frequency-doubled pulses from a 30 Hz Q-switched pulsed Nd:YAG laser (Spectra Physics, model DCR-2A) to generate around 400 fs nearly transform-limited pulses with an energy of 0.4 mJ at 602 nm. A peak power density of around  $400 \text{ MW cm}^{-2}$  was used in our study. The beams in the forward wave geometry for DFWM were focused onto the film. The four-wave mixing signal was detected by a photodiode and processed by a boxcar averager (EG&G Princeton Applied Research, model 4200).

### *Thermal analysis*

Characterization of the thermal elimination reaction of the polymer and composite was performed using a Du Pont 9900 thermogravimetric analyser and d.s.c. These measurements were carried out at the same heating rate ( $20^\circ\text{C min}^{-1}$ ) and under nitrogen atmosphere.

### *Conductivity measurements*

Conductivity was measured using a four-probe configuration by attaching four platinum electrodes across the width of a rectangular piece of polymer or the composite film (cut to  $\sim 15 \text{ mm} \times 8 \text{ mm}$ ) using a conductive colloidal silver adhesive. Four-probe resistance measurements were made using a Keithley model 614 digital multimeter. The  $\text{AsF}_5$  gas was purchased from Matheson Gas Products Inc. and stored in a small gas cylinder which could be attached to the four-probe chamber using a special glass-metal transition connector. All doping and handling of  $\text{AsF}_5$  were performed using a vacuum line under a hood. Conductivity,  $\sigma$ , was calculated by normalizing  $R_s$  by the sample dimensions between the two inner probes as  $\sigma(1/R_s)(l/wt)$ . The film width,  $w$ , and the length between the inner two electrodes,  $l$ , varied from sample to sample. The film thickness,  $t$ , averaged  $\sim 1 \mu\text{m}$ . The sample resistance was monitored during the doping process and was recorded as a function of time. Typically, a sample was doped continuously for up to 7 days until no decrease in resistance was noted over a period of 24 h indicating that the maximum conductivity had been achieved.

## RESULTS AND DISCUSSION

There are several important factors in the preparation of such polymer/silica composites using the sol-gel technique: type of alkoxide used; proper control of pH; the amount of water in the system; type of solvent used in the precursor polymer; reaction temperature; and consolidation temperature. Due to the different properties of the polymer precursor and the alkoxide, the preparation of these composites is greatly affected by these factors and becomes more complicated than for a pure sol-gel system. Improper control of any of the preparation parameters can easily lead to phase separation or precipitation. The results of our study show that the BrMPPV precursor was mixed with silica successfully using the sol-gel process without any phase separation. High optical quality films can be obtained.

Essentially, four stages are involved in the formation of the pure sol-gel system: hydrolysis of TMOS; polymerization of monomer to form small particles; increase in size of the particles; and the linking of these particles to form three-dimensional networks. The polymerization reaction can be pictured as the condensation of the silanol group (reaction I).



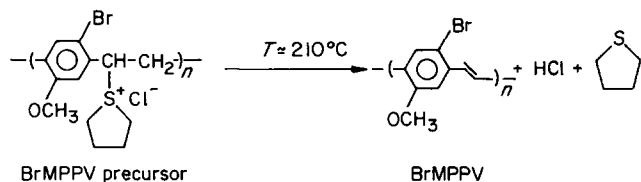
However, in our approach, the precursor polymer is introduced into the sol-gel system, and another reaction is involved to convert the precursor polymer into polymer. In both cases the reactions are E1cB elimination reactions.

*BrMPPV/sol-gel composite*

Since fluidity is important for high optical quality film casting, it is necessary to prolong the gelation time. In order to delay the gelation time of the precursor solution, a known amount of formic acid was added to the system. This formic acid also acted as a catalyst for polymerization of TMOS. The preferable pH value is  $\sim 3$  in this case.

The precursor of BrMPPV is heated at 220°C in a vacuum oven when it undergoes the following E1cB elimination reaction (reaction II) to produce the conjugated polymeric structure of BrMPPV.

Reaction II:



In the BrMPPV/sol-gel densification process, reactions I and II occur simultaneously. As a result, the polymer/sol-gel composite is formed. Since the glass formed in the sol-gel process is porous, the polymer is believed to be embedded within the inorganic oxide glass. However, the pore radii are much smaller (1.5–10 nm)<sup>19</sup> than the near-u.v. or visible radiation wavelength. Consequently, the pure sol-gel glass is transparent<sup>12</sup> and BrMPPV/silica composite exhibits optical quality. Furthermore, an initial study of interference patterns with multiple beam interferometry shows better film homogeneity and smooth surfaces in the sol-gel composites.

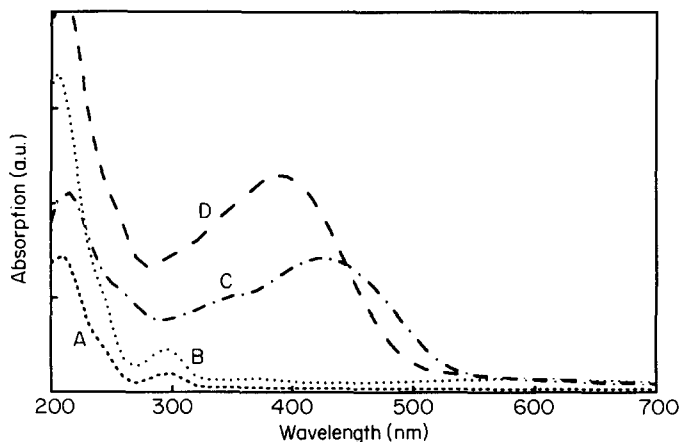


**Figure 1** U.v.-visible absorption spectra of (A) the BrMPPV precursor, (B) the BrMPPV/sol-gel precursor, (C) BrMPPV and (D) the BrMPPV/sol-gel composite

*U.v.-visible spectra.* In Figure 1, curves A, B, C and D show u.v.-visible spectra of the BrMPPV precursor, the BrMPPV/sol-gel silica precursor, polymer BrMPPV and the BrMPPV/sol-gel silica composite, respectively. The precursor films show very weak absorptions in the visible range, indicating that the precursor polymers are very stable at room temperature. The u.v. spectra of the precursor films displayed three absorption bands with overlapping maxima associated with the phenyl group ( $\lambda=210$  nm), the sulphonium group ( $\lambda=265$  nm) and a small bathochromically shifted *trans*-stilbene group ( $\lambda=298$  nm). After the films were thermally eliminated and fully converted the spectra showed a broad, continuous absorption indicative of a highly conjugated system. The onset of the absorption which gives the optical band gap is at 525 nm (2.37 eV) in BrMPPV. The onset is  $\sim 10$  nm blue shifted in the BrMPPV/sol-gel silica composite. The absorption maximum in BrMPPV is 441 nm compared to 395 nm in the BrMPPV/sol-gel composite. This trend is similar to our previous results on PPV and PPV/sol-gel silica composites<sup>12</sup>. This result indicates that polymer chains are indeed incorporated within the bulk of the glass and the effective conjugation length is reduced compared to the BrMPPV polymer.

*I.r. transmission spectroscopy.* The i.r. transmission spectra of the sol-gel silica, BrMPPV and the BrMPPV/sol-gel silica composite are shown in Figures 2A, B and C, respectively. In the spectrum of the sol-gel silica, three characteristic absorption bands of amorphous silica are observed between  $400\text{ cm}^{-1}$  and  $1300\text{ cm}^{-1}$ . The strong band at  $1080\text{ cm}^{-1}$  corresponds to the stretching vibration of the Si-O band<sup>20</sup>. The band at  $455\text{ cm}^{-1}$  is attributed to the vibrational modes of deformation of the O-Si-O and Si-O-Si bonds<sup>20,21</sup>. The band at  $820\text{ cm}^{-1}$  corresponds to the ring structure<sup>22</sup> of the tetrahedral SiO<sub>4</sub>. There are three other bands that appear in the i.r. spectrum of the sol-gel silica at  $3500$ ,  $1620$  and  $950\text{ cm}^{-1}$ . The bands at  $3500$  and  $1620\text{ cm}^{-1}$  correspond to the stretching and deformation modes for hydroxyl groups and water molecules<sup>23</sup>. The absorption band at  $950\text{ cm}^{-1}$  is usually due to the vibration of the Si-O<sup>-</sup> bonds for the glasses containing non-bridging oxygens<sup>24</sup>. In the case of the silica gel it is preferable to attribute this band to the stretching mode of Si-O(OH) bonds<sup>25</sup>. Since this band disappears at higher temperature, it is in good agreement with the evolution of this band during the heat treatment of the gel<sup>26</sup>.

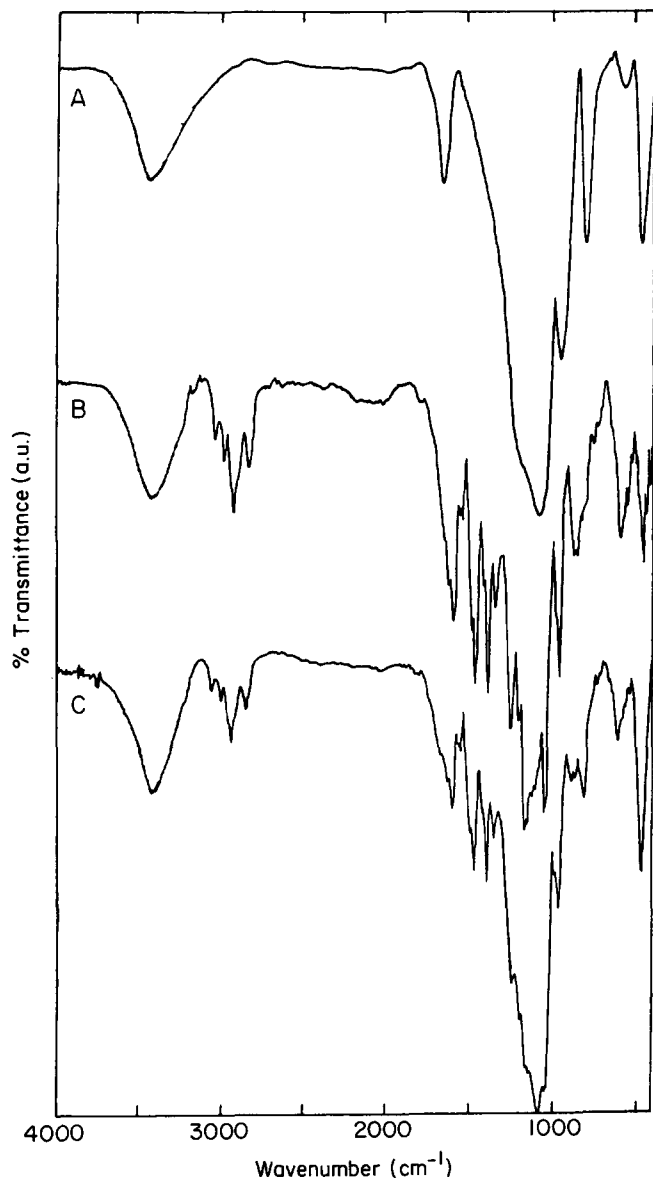


**Figure 2** I.r. transmission spectra of (A) thermally treated (210°C) sol-gel silica, (B) BrMPPV and (C) the BrMPPV/sol-gel silica composite

In the case of fully converted BrMPPV (*Figure 2B*), the *trans*-vinylene CH out-of-plane bending band at  $963\text{ cm}^{-1}$  and *trans*-vinylene C-H stretching<sup>27</sup> at  $3054\text{ cm}^{-1}$  showed up in the i.r. spectrum. No absorbance was observed near  $630\text{ cm}^{-1}$  where the *cis*-CH bending mode would be expected. The i.r. spectrum evidenced a perfect elimination conversion to the polymer BrMPPV.

Finally, the i.r. transmission spectrum of the BrMPPV/sol-gel silica composite (*Figure 2C*) has the features of both sol-gel silica and BrMPPV. This implies that the elimination reaction of BrMPPV does not change in the composite during the sol-gel process.

**Thermal analysis.** D.s.c. and t.g.a. were used to measure the physical, chemical and enthalpic changes which accompanied gel or composite densification. *Figure 3* shows the d.s.c. traces of BrMPPV, the silica gel and the BrMPPV composite precursor which had been dried in a desiccator for 3 months. In the case of BrMPPV (*Figure 3A*), an endothermic effect indicating a combination of the loss of organic volatiles and the E1cB elimination reaction is seen between  $60^\circ\text{C}$  and  $175^\circ\text{C}$ . In

the case of sol-gel silica (*Figure 3B*), an endothermic peak is observed in the range  $50\text{--}210^\circ\text{C}$  which is opposite to the result obtained when the heating process is carried out in the atmosphere (an exothermic response is observed)<sup>28</sup>. This is attributed to the oxidation involving the solvent, or to the oxidation of by-products formed in this range. However, in our case, an inert gas was used and the sol-gel reaction is isolated. The measured endotherm in the range  $50\text{--}150^\circ\text{C}$  is the contribution from dehydration and viscous sintering. *Figure 3C* shows a broadened endothermic response between  $50^\circ\text{C}$  and  $130^\circ\text{C}$  and the peak maximum is lower than that of BrMPPV in *Figure 3A* (from  $120$  to  $90^\circ\text{C}$ ). The shifted peak position provides further evidence for the interaction of the two components (BrMPPV and silica) in the system. The t.g.a. results are consistent with the d.s.c. data. *Figures 4a, b* and *c* show the t.g.a. curves of the BrMPPV precursor, the sol-gel silica and the BrMPPV/sol-gel silica composite, respectively. The corresponding lower curves in *Figures 4a, b* and *c* are the first derivative of the upper curves of the weight loss as a function of temperature. The maxima of the curves showed that the maximum rate of weight loss occurs at  $137$  and  $480^\circ\text{C}$  in BrMPPV (*Figure 4a*). The first transition temperature corresponds to the E1cB elimination of tetrahydrothiophine and some other organic

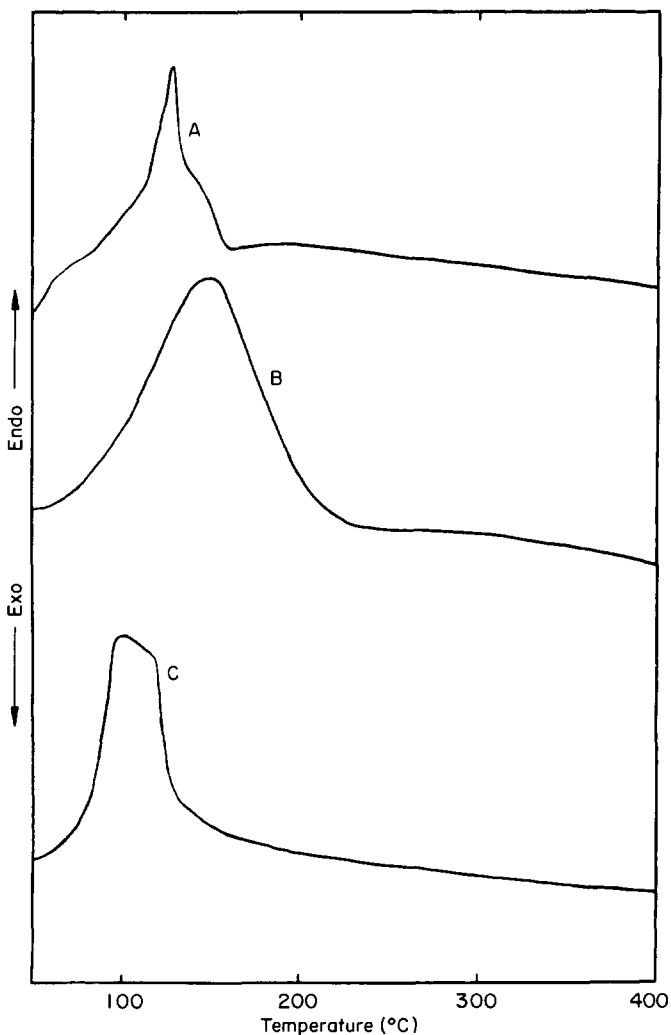


**Figure 3** D.s.c. curves for (A) BrMPPV, (B) sol-gel silica and (C) the BrMPPV/sol-gel silica composite

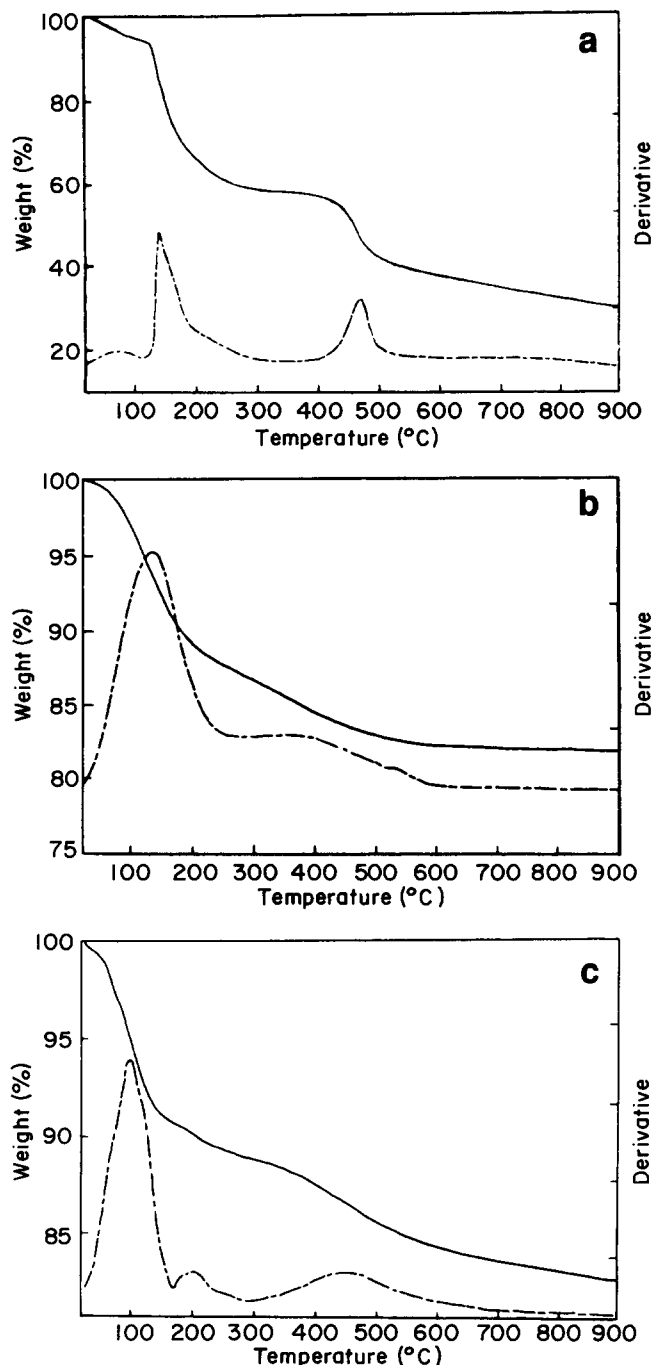


**Figure 4** Thermogravimetric analysis (—) and its first derivative (---) of (a) the BrMPPV precursor, (b) sol-gel silica and (c) the BrMPPV/sol-gel silica composite

solvents. The second transition is the degradation of BrMPPV to a black graphite film. However, in the BrMPPV/sol-gel composite, the transition maxima shifted to 110 and 462°C (Figure 4c) and became broader than in the pure polymer system. All these characteristic features are attributed to a lowering of the activation energy during the condensation-polymerization and sintering of the BrMPPV/sol-gel silica composite. Furthermore, the repeat scan shows that the process associated with the endothermic reaction is irreversible and no glass transition is detected.

#### BuMPPV/sol-gel composite

The preparation of the BuMPPV/sol-gel composite is similar to that of the BrMPPV/sol-gel composite. The

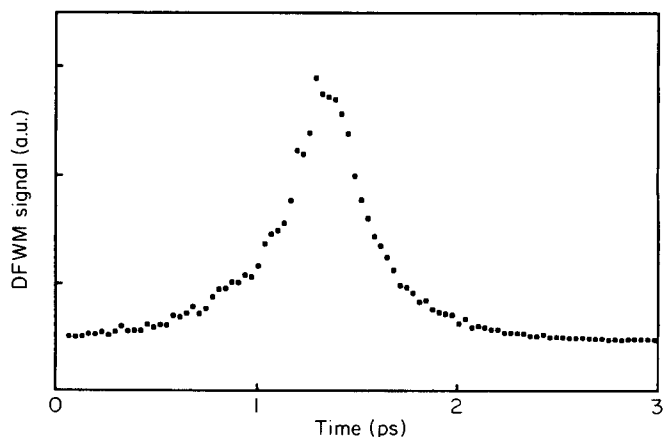
only difference in preparation of the BuMPPV/sol-gel composite is that tetrahydrofuran (THF) is used as the common solvent instead of methanol. However, the u.v.-visible and i.r. spectra as well as thermal properties showed similar characteristics in the BuMPPV/sol-gel silica composite. The results of the  $\chi^{(3)}$  measurements are compared and analysed in the following.

**Energy band gaps and  $\chi^{(3)}$  measurements.** The  $\chi^{(3)}$  value was evaluated by comparing the strength of the signal at low incident photon flux with that of CS<sub>2</sub> according to the following relationship<sup>1</sup>:

$$\frac{\chi_s^{(3)}}{\chi_c^{(3)}} = \left(\frac{n_s}{n_c}\right)^2 \frac{l_c}{l_s} \left(\frac{I_s}{I_c}\right)^{1/2} \left\{ \frac{\alpha l_s}{\exp(-\alpha l_s/2)[1 - \exp(-\alpha l_s)]} \right\} \quad (1)$$

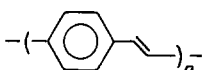
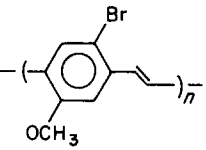
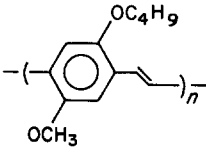
where  $n$  is the refractive index,  $l$  is the interaction length and  $\alpha$  is the linear absorption coefficient. The subscripts  $c$  and  $s$  refer to CS<sub>2</sub> and the sample, respectively. The CS<sub>2</sub> sample is non-absorbing at the wavelength used. The value of  $\chi^{(3)} = 6.8 \times 10^{-13}$  esu was used as the reference value<sup>29</sup> for CS<sub>2</sub>. However, in the case of BrMPPV the absorption term in equation (1) is ignored because the sample is nearly non-resonant at 602 nm (Figure 1). The measured effective  $\chi^{(3)}$  values for BrMPPV and BuMPPV are  $\sim 9 \times 10^{-10}$  and  $\sim 10^{-9}$  esu, respectively. The subpicosecond DFWM response of BrMPPV is shown in Figure 5. These values can be compared with that of  $\sim 4 \times 10^{-10}$  reported by Singh *et al.*<sup>30</sup> for PPV at 602 nm. The  $\chi^{(3)}$  values for the polymer/sol-gel silica composites show slightly smaller values than for the corresponding pure polymer. Based on the number density consideration ( $\sim 50$  wt% polymer in the composite), a reduction in the  $\chi^{(3)}$  value by a factor of 2 would be expected. The observation that the composite film shows a  $\chi^{(3)}$  value very close to that of the parent polymer film may be a consequence of the significantly improved optical quality of the composite film permitting a more realistic assessment of its intrinsic  $\chi^{(3)}$  value. A similar situation has been found in another polymer composite of poly(*p*-phenylene-benzobisthiazol) and nylon (Zytel 330), where the improved optical quality of the film yielded a higher  $\chi^{(3)}$  value<sup>31</sup>.

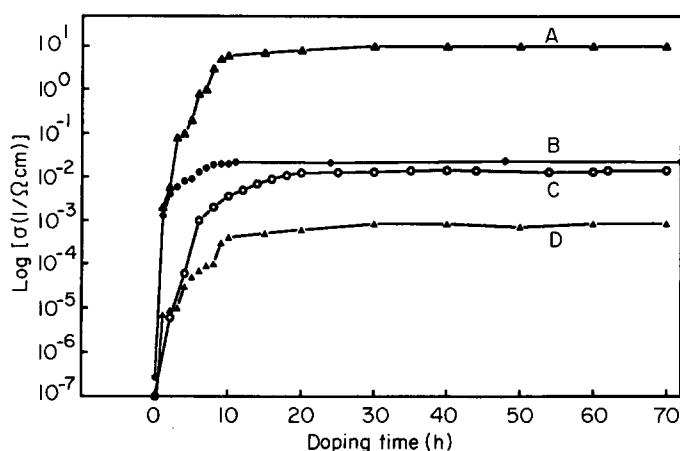
Organic polymeric structures with extensive  $\pi$ -conjugation have a relatively large  $\chi^{(3)}$  value, which is derived from the  $\pi$ -electron delocalization<sup>1</sup>. The trend of our measurement reflects the contribution of the electron



**Figure 5** DFWM signal observed for BrMPPV as a function of the forward beam delay. The wavelength is 602 nm and the pulses are  $\sim 400$  fs wide

**Table 1** Structures of PPV and its derivatives, band gap energies and  $\chi^{(3)}$  values

Structures	Materials	Band gap energies (eV)	$\chi^{(3)}$ (esu)
	PPV film	2.46	$\sim 4 \times 10^{-10}$
	PPV/sol-gel silica composite	2.70	$\sim 3 \times 10^{-10}$
	BrMPPV film	2.37	$\sim 9 \times 10^{-10}$
	BrMPPV/sol-gel silica composite	2.52	$\sim 8 \times 10^{-10}$
	BuMPPV film	2.19	$\sim 1 \times 10^{-9}$
	BuMPPV/sol-gel silica composite	2.23	$\sim 1 \times 10^{-9}$

**Figure 6** Electrical conductivities of  $\text{AsF}_5$  doped (A) PPV, (B) PPV/sol-gel silica, (C) BrMPPV and (D) BrMPPV/sol-gel silica

donor substituents at the 2 and 5 positions of PPV. The butoxy and methoxy electron donor groups at the 2 and 5 positions enhance the  $\pi$ -electron density in the conjugated polymer BuMPPV. The energy band gap is smallest and the effective  $\chi^{(3)}$  value is the largest for BuMPPV. The structures of PPV and its derivatives, band gap energies and  $\chi^{(3)}$  values are presented in Table 1.

**Electrical conductivity.** Uniaxial orientation of films are known to significantly improve electrical conductivity along the stretching direction<sup>32,33</sup>. Studies of doped PPV show that conductivities approaching those obtained for doped polyacetylene are achievable. The maximum conductivity<sup>16</sup> of fully eliminated PPV films doped with dopant  $\text{AsF}_5$  is  $10 \text{ S cm}^{-1}$ . On the other hand, the only known conductivities of BrMPPV are those for iodine doped stretched films. The films with stretching ratios of 1 and 6 had conductivities of  $7.4 \times 10^{-5}$  and  $2.5 \times 10^{-3} \text{ S cm}^{-1}$ , respectively<sup>18</sup>. Figure 6 shows the electrical conductivities of  $\text{AsF}_5$  doped PPV, PPV/sol-gel silica, BrMPPV and BrMPPV/sol-gel silica. Our results show that the  $\text{AsF}_5$  doped PPV/sol-gel film has a maximum conductivity of  $0.023 \text{ S cm}^{-1}$  and the  $\text{AsF}_5$

doped unstretched BrMPPV and BrMPPV/sol-gel silica films have maximum conductivities of  $1.4 \times 10^{-2}$  and  $8.3 \times 10^{-4} \text{ S cm}^{-1}$ , respectively. The conductivity of the polymer/silica glass composite is smaller than that of the pure polymer films.

## CONCLUSIONS

The BrMPPV and BuMPPV polymers have been mixed successfully with silica using the sol-gel technique. These materials have been characterized using u.v.-visible, FTi.r. spectra and thermal analyses. The blue shift in the u.v.-visible spectra and shifted peak positions in the d.s.c. response provide strong evidence of interaction between the polymer and the silica components. The  $\chi^{(3)}$  values of PPV and its derivatives as well as the polymer/sol-gel silica composites have been determined using the DFWM technique. The increased third-order non-linearities of the substituted PPV polymer indicate important effects of electron donor substituents at the 2 and 5 positions in PPV. Even though the  $\chi^{(3)}$  values are slightly lower in the polymer/sol-gel silica composites, the sol-gel processed polymer/silica films are of significantly improved optical quality than the pure polymers.

## ACKNOWLEDGEMENTS

The research work at the Photonics Research Laboratory is supported in part by the Air Force Office of Scientific Research, Directorate of Chemical and Atmospheric Sciences and Polymer Branch, Air Force Wright Laboratory, through contract number F49620-90-C-0021 and in part by the Office of Innovative Science and Technology-Defense Initiative Organization/Air Force Office of Scientific Research through contract number F49620-91-C0053.

The authors wish to thank the Korea Research Institute of Chemical Technology for providing two four-probe chambers for electrical conductivity measurements. We also wish to thank Dr Marek Samoc for useful discussions and comments.

## REFERENCES

- Prasad, P. N. and Williams, D. J. 'Introduction to Nonlinear Optical Effects in Molecules and Polymers', Wiley, New York, 1991
- Prasad, P. N. and Ulrich, D. R. (Eds) 'Nonlinear Optical and Electroactive Polymers', Plenum Press, New York, 1988
- Williams, D. J. (Ed.) 'Non-Linear Optical Properties of Organic and Polymeric Materials', American Chemical Society, Washington, DC, 1983
- Clymer, B. and Collins Jr, S. A. *Opt. Eng.* 1985, **24**, 74
- Mackenzie, J. D. in 'Ultrastructure Processing of Ceramics, Glasses and Composites' (Eds L. L. Hench and D. R. Ulrich), Wiley, New York, 1984, p. 15
- Uhlmann, D. R., Zelinski, B. J. J. and Wnek, G. E. in 'Better Ceramics through Chemistry' (Eds C. J. Brinker, D. E. Clark and D. R. Ulrich), Vol. 32, Materials Research Society, North-Holland, New York, 1985, p. 59
- Brinker, C. J. and Scherer, G. W. 'Sol-Gel Science, The Physics and Chemistry of Sol-Gel Processing', Academic Press, New York, 1990, Ch. 14
- Mackenzie, J. D. *J. Non-Cryst. Solids* 1982, **48**, 1
- Dislich, H. and Hinz, P. *J. Non-Cryst. Solids* 1982, **48**, 11
- Segal, D. L. *J. Non-Cryst. Solids* 1984, **63**, 183
- Prasad, P. N., Karasz, F. E., Yang, Y. and Wung, C. J. *US Pat. Appl.* 312132, 1989
- Wung, C. J., Pang, Y., Prasad, P. N. and Karasz, F. E. *Polymer* 1991, **32**, 605

- 13 He, G. S., Wung, C. J., Xu, G. and Prasad, P. N. *Appl. Optics* 1991, **30**, 3810
- 14 Burzynski, R., Rao, D. N. and Prasad, P. N. unpublished results
- 15 Pang, Y., Samoc, M. and Prasad, P. N. *J. Chem. Phys.* 1991, **94**, 5282
- 16 Gagnon, D. R., Capistran, J. D., Karasz, F. E., Lenz, R. W. and Antoun, S. *Polymer* 1987, **28**, 567
- 17 Jin, J. I., Park, C. K., Shim, H. K. and Park, Y. W. *J. Chem. Soc., Chem. Commun.* 1989, 1205
- 18 Chi-Kyun Park, Hong-Ku Shim and Jung-Il Jin, unpublished results
- 19 Yamane, M., Aso, S. and Sakaino, T. *J. Mater. Sci.* 1978, **13**, 865
- 20 Lippencott, E. R., Van Valkenburg, A., Weir, C. E. and Bunting, E. N. *J. Res. Natl Bur. Std* 1958, **61**, 61
- 21 Hanna, R. *J. Am. Ceram. Soc.* 1965, **48**, 595
- 22 Kamiya, K. and Sakka, S. *Res. Rep. Fac. Eng. Mie Univ.* 1977, **2**, 87
- 23 Fripiat, J. and Jelli, A. *Congre Int. du verre, Bruxelles*, 1968, p. 14
- 24 Mukherjee, S. P. *J. Non-Cryst. Solids* 1980, **42**, 477
- 25 Zarzycki, J. and Naudin, F. *J. Chim. Phys.* 1961, **58**, 830
- 26 Decottignies, M., Phalippou, J. and Zarzycki, J. *J. Mater. Sci.* 1978, **13**, 2605
- 27 Tokito, S., Momii, T., Murata, H., Tsutsui, T. and Saito, S. *Polymer* 1990, **31**, 1137
- 28 Carturan, G., Gottardi, V. and Graziani, M. *J. Non-Cryst. Solids* 1978, **29**, 41
- 29 Xuan, N. P., Ferrier, J. L., Gazengel, J. and Rivorie, G. *Opt. Commun.* 1984, **51**, 433
- 30 Singh, B. P., Prasad, P. N. and Karasz, F. E. *Polymer* 1988, **29**, 1940
- 31 Lee, C. Y.-C., Swiatkiewicz, J., Prasad, P. N., Mehta, R. and Bai, S. J. *Polymer* 1991, **32**, 1195
- 32 Han, C. C., Lenz, R. W. and Karasz, F. E. *Polym. Commun.* 1987, **28**, 26
- 33 Jen, K. Y., Shacklette, L. W. and Elsenbaumer, R. *Synth. Met.* 1987, **22**, 179